

# Methane Partial Oxidation over Vanadyl Pyrophosphate and the Effect of Fe and Cr Promoters on Selectivity

Robert L. McCormick,<sup>\*,1</sup> Gokhan O. Alptekin,<sup>\*</sup> Andrew M. Herring,<sup>\*</sup> T. R. Ohno,<sup>†</sup> and Steven F. Dec<sup>‡</sup>

<sup>\*</sup>Department of Chemical Engineering and Petroleum Refining, <sup>†</sup>Department of Physics, and <sup>‡</sup>Department of Chemistry and Geochemistry, Colorado School of Mines, Golden, Colorado 80401-1887

Received April 4, 1997; revised July 23, 1997; accepted July 24, 1997

Partial oxidation of methane by molecular oxygen over Cr- and Fe-promoted, as well as unpromoted, vanadyl pyrophosphate catalysts has been studied in the temperature range of 573–698 K and atmospheric pressure. Carbon monoxide, carbon dioxide, and water were found to be the principal reaction products over unpromoted vanadyl pyrophosphate. Over both the Fe- and Cr-promoted catalysts high formaldehyde selectivity was observed at very low methane conversion levels with HCHO space time yields in the range of 0.5 to 2.0 g/kg-h. As the extent of the reaction was increased selectivity to formaldehyde decreased rapidly and changes in selectivities with conversion indicate a sequential conversion of methane to formaldehyde, CO, then CO<sub>2</sub>. Macrokinetic parameters for the methane oxidation reaction were determined for the unpromoted catalyst. A simple power law rate expression fit the rate data well over the whole temperature range. The rate of reaction of methane was  $0.08 \pm 0.02$  order in oxygen partial pressure,  $0.73 \pm 0.07$  order in methane partial pressure, and the activation energy was found to be  $102 \pm 6$  kJ/mole. Activation energy was unchanged by promotion with Fe and Cr. Analysis by XPS and ICP-AA indicates that promoters were incorporated equally into the bulk and surface of these catalysts. XPS indicates an increase in the average surface oxidation state of vanadium in the promoted catalysts and XRD shows that promotion causes oxidation of a small fraction of the pyrophosphate to form  $\alpha_{II}$ -VOPO<sub>4</sub>. <sup>31</sup>P NMR spin-echo mapping confirms the enhanced formation of V<sup>5+</sup> in the promoted samples. The presence of V<sup>5+</sup> may therefore be required for the formation of selective products. It is proposed that the role of promoters is to increase the rate of formation of V<sup>5+</sup> during activation, or to stabilize V<sup>5+</sup> containing domains under the highly reducing methane oxidation conditions. © 1997 Academic Press

## INTRODUCTION

Methane partial oxidation to methanol and formaldehyde is one of the most difficult challenges in catalysis. Severe reaction conditions are required to activate this otherwise very stable species, and under such conditions the desired oxygenates can be oxidized to CO<sub>x</sub> and water. Partial

oxidation reactions of methane to methanol and formaldehyde are thermodynamically favorable ( $\Delta G^\circ = -291, -111$  kJ/mole, respectively), but combustion products are more so ( $\Delta G^\circ = -544, -801$  kJ/mole for CO and CO<sub>2</sub>, respectively). Thermodynamic instability of the desired products with respect to those of combustion requires a catalyst and reaction conditions that facilitate the formation of oxygenates without oxidizing them further. A large number of catalysts have been studied in the literature, with most of the attention focused on molybdenum and vanadium-based systems. Several reviews (1–4) have been published in recent years and provide an overall view of the progress made in this field. High selectivities toward the desired products are usually achieved only at very low methane conversion and yields are too low to be of economic interest.

Vanadyl pyrophosphate, with the formula (VO)<sub>2</sub>P<sub>2</sub>O<sub>7</sub> (referred to as VPO in this paper), combined with related V–P–O phases is used commercially to catalyze the selective oxidation of *n*-butane to maleic anhydride (5). Pure vanadyl pyrophosphate contains only V<sup>IV</sup> but the presence of V<sup>V</sup> is required for selective hydrocarbon oxidation to proceed (6) and to complete the V<sup>IV</sup>/V<sup>V</sup> redox couple. The exact state of V<sup>V</sup> in these materials (i.e., isolated surface sites or macroscopic domains of a specific phosphate phase) is an area of active research (7–11). It is clear, however, that the most active and selective catalysts are largely composed of vanadyl pyrophosphate (11, 12). VPO exhibits a unique ability to activate and selectively oxidize alkanes. There are published reports on VPO indicating moderate to high selectivity in oxidation of ethane (13), propane (14) and pentane (15), as well as butane (5). It has been shown that for saturated hydrocarbons, the first step in activating the molecule is the dissociation of the C–H bond in a manner similar to the production of hydrocarbon free radicals (16). Strong Lewis acid sites present on the surface of VPO may initiate alkane activation (17). Vanadyl pyrophosphate undergoes a phase change to VOPO<sub>4</sub> at temperatures above 773 K in the presence of oxygen (18). Five polymorphs of VOPO<sub>4</sub> are known. Methane oxidation, over what was probably  $\alpha_1$ -VOPO<sub>4</sub>, has been investigated by

<sup>1</sup> To whom correspondence should be addressed. E-mail: rlmccorm@mines.edu.

Lopez Granados and Wolf (19) and formation of formaldehyde at low yield was reported in the temperature range 873–993 K.

In the work reported here we have examined vanadyl pyrophosphate for activity and selectivity in the methane partial oxidation reaction at atmospheric pressure and in the temperature range 573–698 K. A variety of cations have been added to vanadium phosphate catalysts to improve catalyst activity or selectivity (20). For *n*-butane oxidation beneficial effects have been claimed for promotion by many of the first row transition metals (20–24), although negative effects have also been observed (24). Vanadyl pyrophosphate promoted with Fe and Cr has also been examined for the methane partial oxidation reaction in this work.

## METHODS

### Catalyst Preparation

**Unpromoted VPO catalyst.** Vanadyl pyrophosphate was prepared following the procedure reported by Busca and co-workers (25). Fifteen grams of  $V_2O_5$  was suspended in 90 ml of isobutyl alcohol and 60 ml of benzyl alcohol. The suspension was stirred under reflux for 3 h, then cooled to room temperature and left stirring overnight. Then 16.2 g 99% anhydrous phosphoric acid was added (P : V atomic ratio 1.00), and the mixture was refluxed for an additional 2 h. After completion of the reaction, the solid phase was recovered by filtration, washed with isobutyl alcohol, and dried in air at 393 K overnight. The dried catalyst precursor,  $VOHPO_4 \cdot 0.5H_2O$ , was then calcined in 1.5% butane in air at 673 K for 18 h ( $GHSV\ 800\ h^{-1}$ ) to facilitate the transformation to vanadyl pyrophosphate.

**Promoted VPO catalysts.** Nitrate salts of Cr and Fe were used as the source of promoter elements. Five grams of  $Cr^{III}$  nitrate nonahydrate or 5.05 g of  $Fe^{III}$  nitrate nonahydrate was dissolved in a benzyl/isobutyl alcohol mixture. This was then added to 45 g of previously prepared precursor that had been resuspended under reflux in a benzyl/isobutyl alcohol mixture and cooled. This mixture was then stirred at 323 K overnight. The precipitate was then filtered and washed with more solvent and dried in a rotary vacuum drier for 8 h at slightly greater than ambient temperature. The promoted catalyst precursors were activated in the same way described for unpromoted VPO.

### Analytical Methods

Specific surface areas (BET) of the catalyst samples were measured using a Micromeritics 2100E Accusorb Instrument. Nitrogen was used as adsorbate at liquid nitrogen temperatures, taking a value of  $0.162\ nm^2$  for the cross section area of the adsorbed nitrogen molecule. X-ray powder diffraction (XRD) patterns were obtained using a Rigaku diffractometer.  $Cu\ K_\alpha$  radiation ( $\lambda = 1.5432\ \text{\AA}$ ) was used as the incident X-ray source. Infrared spectra were obtained

by diffuse reflectance on a BioRad FTS-40 instrument using a Harrick diffuse reflectance attachment and samples mixed with KBr. Chemical analysis was performed by ICP-AA on samples digested in concentrated nitric acid and then diluted before analysis. A Kratos Electronics spectrometer with monochromatic  $Al\ K_\alpha$  radiation was used to obtain the X-ray photoelectron spectra (XPS). The binding energy of  $C\ 1s$  (284.6 eV) was used as a reference in these measurements. Deconvolution of the  $V\ 2p_{3/2}$  binding energy envelope was performed by fitting two Gaussian peaks separated by 1 to 1.1 eV with a nonlinear regression package varying intensity and peak width. Wide-line (nonspinning)  $^{31}P$  NMR experiments were conducted on a Chemagnetics CMX Infinity 400 instrument (7.5 mm probe,  $^{31}P$  spectral frequency of 162.0 MHz) using a spin-echo mapping approach similar to that described by Li and co-workers (7). In our implementation of this method the carrier frequency was varied in increments of 62.5 kHz above and below the resonance frequency of  $^{31}P$  in 85%  $H_3PO_4$  to cover the complete range where spectral intensity was observed.

### Catalyst Testing

Steady-state reaction studies were performed in a fixed-bed micro-reactor. The composition ( $CH_4$ ,  $O_2$ , He) and flow rate of the feed gas was controlled by Brooks 5850E mass flow controllers. The reactor was a quartz tube, 30-cm long and 1.0-cm ID at the catalyst bed portion, mounted vertically in a tubular furnace. A quartz frit was used to hold the catalyst bed in place. Typically about 0.3 g of catalyst (screened to 0.5–0.7 mm particle size,  $0.677\ g/cm^3$  bulk density) was loaded into the reactor and covered with 15-mm layer of quartz beads to obtain a preheating zone and a uniform gas distribution. The exit diameter was decreased to 5-mm ID right after the quartz frit to allow reaction products to leave the heated zone more rapidly. Temperature was monitored by two K-type thermocouples, one placed in contact with the catalyst bed and the other right under the frit. Prior to reaction the catalyst was calcined *in situ* under helium flow (20 ml/min) at the reaction temperature for 1 h. Methane was introduced into the reactor first so that at all times the methane–oxygen mixture was kept well above the upper explosive limits. Methane conversion was well below 10% for all experiments reported. Overall carbon balance closures obtained were within  $\pm 5\%$  and mostly within  $\pm 3\%$ . Fractional conversion and selectivity were defined as

$$\text{Conversion} = \frac{\text{moles (HCHO + CO + CO}_2\text{) formed}}{\text{moles CH}_4\text{ fed}}$$

$$\text{Selectivity} = \frac{\text{moles product formed}}{\text{moles (HCHO + CO + CO}_2\text{) formed}}$$

An on-line Hewlett-Packard 5890 Gas Chromatograph (GC) equipped with a thermal conductivity detector was

used to analyze reactant and product streams. Separation of  $\text{CH}_4$ ,  $\text{O}_2$ ,  $\text{CO}$ , and  $\text{CO}_2$  was accomplished with a  $6 \text{ ft} \times 1/8 \text{ in. S.S. Carbosphere 80/100}$  column. For methanol, formaldehyde, and water an  $8 \text{ ft} \times 1/8 \text{ in. S.S. Poropak-T}$  column was used. For the Carbosphere column a GC temperature program starting at 323 K and ending at 403 K was applied, with an initial soak time of 3 min and a heating rate of 30 K/min. For the Poropak-T column, the GC temperature was held constant at 403 K. Calibration for  $\text{CH}_4$ ,  $\text{CO}$ , and  $\text{CO}_2$  was accomplished using standards from Scott Specialty Gases. Methanol and water calibrations were performed using standard solutions of reagent grade methanol and deionized water prepared in volumetric flasks. Calibration of the GC for formaldehyde is more complex. Paraformaldehyde was placed in a heated flask, purged by the feed gas. A feed gas of oxygen-helium was passed through the system and

analyzed to obtain a formaldehyde peak area. The mixture was then passed over a 4 wt%  $\text{Pd}/\text{Al}_2\text{O}_3$  combustion catalyst at 673 K. Complete formaldehyde conversion was obtained and  $\text{CO}_2$  was the only combustion product. The known  $\text{CO}_2$  calibration was then used to determine the concentration of formaldehyde in the feed gas.

## RESULTS

### *Catalyst Characterization*

X-ray diffraction data obtained for the precursor show the peaks of vanadyl phosphate hemihydrate  $\text{VOHPO}_4 \cdot 0.5\text{H}_2\text{O}$ . A poorly crystalline vanadyl pyrophosphate was the only phase observed by XRD in the activated, unpromoted sample in agreement with the results reported for this preparation method (25) as shown in Fig. 1. Given the

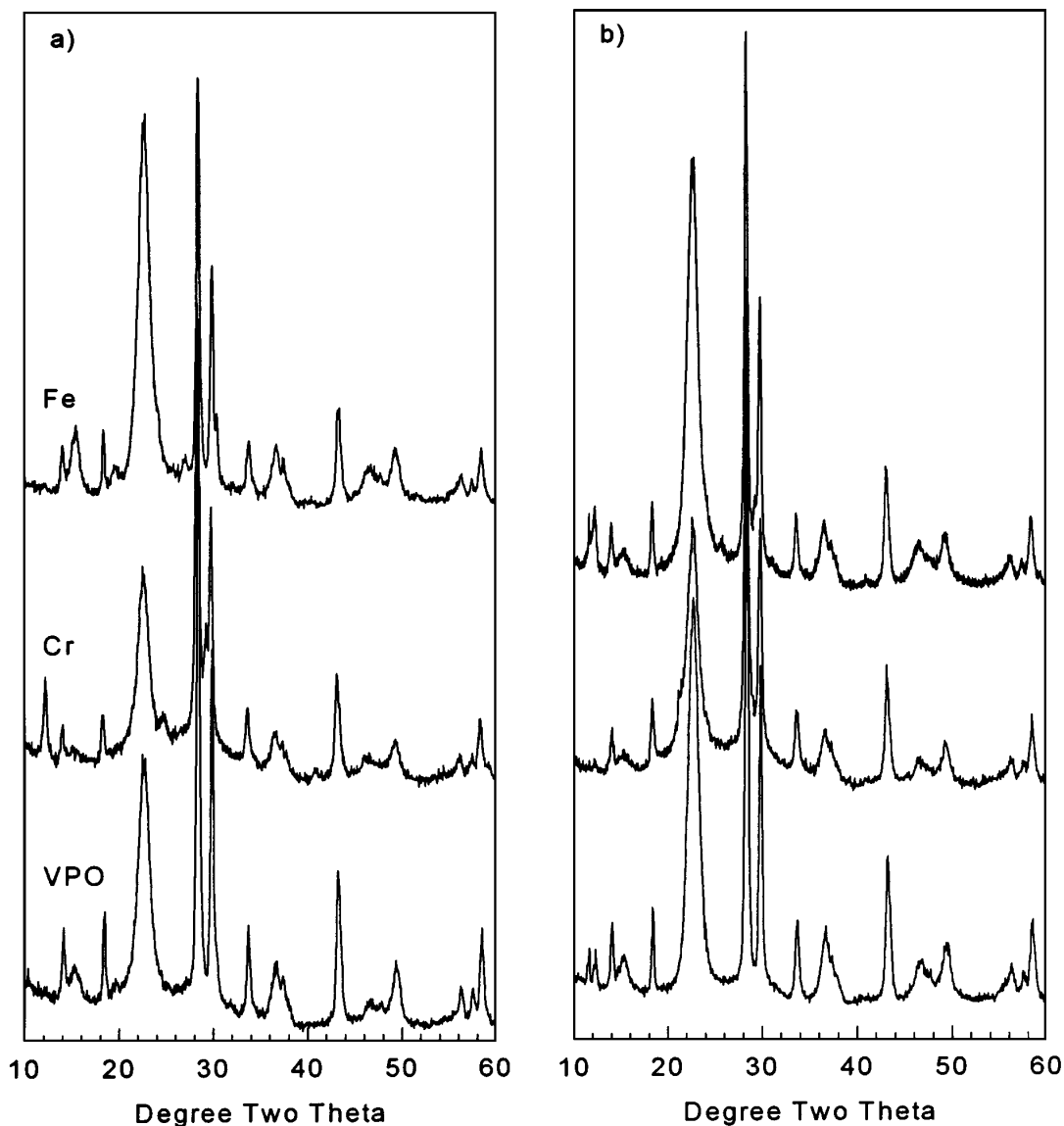


FIG. 1. X-ray diffraction patterns of unpromoted and promoted vanadyl pyrophosphate catalysts.

**TABLE 1**  
**Characterization Results for Vanadyl Pyrophosphate**  
**and Promoted Catalysts**

Catalyst	Surface area (m <sup>2</sup> /g)	Surface promoter: V	Bulk promoter: V	Surface P:V ratio	Bulk P:V ratio
VPO	32.1	—	—	1.23	0.97
Cr-VPO	33.8	0.13	0.08	1.58	0.99
Fe-VPO	32.6	0.09	0.11	1.16	0.92

broadness of some of the XRD peaks the presence of other VPO phases cannot be completely ruled out, however. After exposure to methane oxidation conditions for 20 h the (200) reflection at 22.8° has increased in intensity, suggesting that order in the layer stacking direction has increased.

Figure 1 also reports X-ray diffraction data for both transition metal-promoted VPO catalysts after activation and after use for 20 h in methane oxidation. These data show that additional peaks are evident for Fe- and Cr-promoted VPO. In the Cr-promoted sample, peaks at 24.9° (3.58 Å), 29.15° (3.06 Å), and 40.71° (2.21 Å) in the activated sample correspond to  $\alpha_{II}$ -VOPO<sub>4</sub> (7). The peak at 12.2° (7.26 Å) could not be assigned. These are reduced in intensity after exposure to methane oxidation conditions and a new peak is observed at 21.9° (4.21 Å). The crystallinity of this material does not appear to have developed during catalysis, as relative peak intensities are essentially unchanged. These data indicate that addition of Cr by the method outlined in the experimental section causes the predominantly vanadyl pyrophosphate starting material to be oxidized. For the Fe-promoted sample, peaks at 27.1° (3.29 Å) and 30.4° (2.94 Å) after activation do not correspond to obvious oxide phases of the promoter or of V-P-O. These peaks might correspond to iron phosphates but with only two peaks a definitive assignment cannot be made. After exposure to methane oxidation conditions peaks corresponding to a VOPO<sub>4</sub> phase are observed at 25.8° (3.95 Å), 29.2° (3.06 Å), and 40.7° (2.24 Å). It is notable that the (200) reflection at 22.8° is much more intense in this catalyst following activation

than in the others. After use in methane/oxygen the relative intensity is comparable to that for the unpromoted VPO. These data indicate that Fe promotion enhances the rate of development of crystallinity and suggest that one reason for the use of Fe as a promoter for industrial butane oxidation catalysts (20) is because equilibrium catalysts are more rapidly obtained.

Surface areas are listed in Table 1 and are nearly identical for all three catalysts. XPS results, also in Table 1, indicate that roughly one tenth of the surface metal atoms are promoter. Bulk analysis yields similar results indicating that the method of introducing promoters modifies both the surface and bulk composition. Surface P:V ratios are well above 1.0 as has been reported for commercial butane oxidation catalysts. Bulk P:V ratios are slightly below 1.0 and slightly below the ratio employed in the catalyst synthesis.

XPS binding energies for vanadium (2p<sub>3/2</sub>), phosphorus (2p), oxygen (1s), and the promoter atoms are listed in Table 2. Reported binding energies in the vanadyl pyrophosphate phase (P/V = 1.0–1.2) range from 516.6 to 517.9 eV (26, 27). For reference, V<sup>V</sup> compounds show binding energies of 518.2 eV for  $\beta$ -VOPO<sub>4</sub> (21) and 517.1 eV for V<sub>2</sub>O<sub>5</sub> (26). The binding energy of 516.9 eV reported in Table 2 is in good agreement with literature values when differences in the C 1s reference binding energy are considered. Binding energies in this range were also observed for the promoted catalysts although peaks are significantly broadened. Deconvolution of the V 2p<sub>3/2</sub> peak envelope leads to the average vanadium oxidation state reported in Table 2. Promotion has resulted in oxidation of a significant fraction of the surface vanadium atoms.

An additional method for discerning vanadium oxidation states employs the difference in binding energy of the O 1s and V 2p<sub>3/2</sub> signals ( $\Delta_{O\ 1s-V\ 2p}$ ) which is correlated with the surface oxidation states (26, 28, 29). This approach eliminates the need for a reference binding energy such as C 1s. The binding energy difference for pure vanadyl pyrophosphate, known to contain mostly V<sup>IV</sup>, varies from 14.9 to 15.2 for P/V = 1.0 to 1.2. For the V<sup>V</sup> containing  $\beta$ -VOPO<sub>4</sub> the binding energy difference is between 13.0 to 13.9 and for V<sub>2</sub>O<sub>5</sub> is 12.9 eV (27). This binding energy difference shifts

**TABLE 2**  
**XPS Binding Energies and Estimated Average Vanadium Oxidation State<sup>a</sup> Observed for Promoted**  
**and Unpromoted Catalysts**

Catalyst	V 2p <sub>3/2</sub>	O 1s	P 2p	$\Delta_{O\ 1s-V\ 2p}$	V <sub>ox-Fit</sub>	V <sub>ox-Corr</sub>	V <sub>ox-NMR</sub>
(VO) <sub>2</sub> P <sub>2</sub> O <sub>7</sub>	516.5 (1.9) <sup>b</sup>	532.0 (2.2)	134.1 (1.9)	15.1	4.15	3.55	4.03/4.06
Cr-VPO	517.5 (1.8)	531.4 (1.6)	134.0 (1.8)	13.9	4.22	4.38	4.12/4.12
Fe-VPO	517.4 (2.4)	531.3 (1.8)	134.0 (1.8)	13.9	4.38	4.38	4.00/4.10

<sup>a</sup> V<sub>ox-Fit</sub> is by the deconvolution approach described in the experimental section. V<sub>ox-Corr</sub> is based on the correlation with  $\Delta_{O\ 1s-V\ 2p}$  presented in Ref. (29). V<sub>ox-NMR</sub> is based on integration of the <sup>31</sup>P NMR intensities after activation/and after catalysis of methane oxidation.

<sup>b</sup> Full width at half maximum shown in parenthesis.

towards lower energy values with addition of promoter elements consistent with an increase in the amount of  $V^V$  on the surface. Coulston and co-workers (29) present a correlation vanadium average oxidation state and  $\Delta_{O\ 1s-V\ 2p}$ . This correlation has also been used to estimate the average vanadium oxidation state and these values are reported in Table 2 for comparison with estimates based on deconvolution. The correlated value for the unpromoted catalysts is significantly lower than estimated by our deconvolution approach, and the values for the promoted catalysts are slightly higher. This approach again confirms the difference in average surface oxidation state for the promoted and unpromoted materials.

The  $(VO)_2P_2O_7$  phase reported in the literature (27) yields an O 1s binding energy of 531.1 to 532.8 eV with a narrow signal (FWHM 2.4 eV). More oxidized  $V^V$  phases with and without phosphorus exhibit a much narrower O 1s signal (1.7–2.0 eV), shifted slightly downwards in some cases such as 531.2 ( $\beta$ - $VOPO_4$ ) and 530.0 eV ( $V_2O_5$ ). The data in Table 2 indicate O 1s binding energies comparable to pure  $(VO)_2P_2O_7$  for the unpromoted as well the Fe- and Cr-promoted catalysts. The signal is significantly narrower for the promoted materials consistent with a higher average surface oxidation state for vanadium.

Binding energies for the promoter elements were also examined by XPS. For the Fe-promoted catalyst, the Fe  $2p_{3/2}$  binding energy value of 714.2 eV indicates very little possibility of presence of FeO or  $Fe_2O_3$  on the surface. The Fe  $2p_{3/2}$  energy is 709.5 eV for FeO, 710.8 eV for  $Fe_2O_3$ , and 711.5 eV for  $FeCl_3$ . For Fe promoted vanadyl pyrophosphate the binding energy is much greater. Wang and Otsuka (30) report a similarly high binding energy of 713.2 eV for  $FePO_4$  suggesting the presence of  $Fe^{III}$  in a phosphate matrix in the Fe promoted sample. For  $Cr_2O_3$ , the  $2p_{3/2}$  energy is reported as 578.8 eV. The observed Cr  $2p_{3/2}$  energy of 578.3 eV for the Cr-promoted catalyst is very close to the value of 578.5 reported for  $\beta$ - $CrPO_4$  (31), indicating  $Cr^{III}$  in a phosphate matrix.

Li and co-workers (7) introduced the use of  $^{31}P$  NMR spin-echo mapping to determine the presence of bulk  $V^{IV}$  and  $V^V$  species in vanadium phosphate catalysts. These spectra are characterized by a broad peak centered at about 2500 ppm (relative to  $H_3PO_4$ ) and assigned to phosphorus in the vicinity of  $V^{IV}$ , and a narrower peak near 0 ppm assigned to phosphorus near  $V^V$ . Spectra of promoted and unpromoted samples, both freshly activated and after use in methane oxidation, are shown in Fig. 2. For the activated, unpromoted catalyst there is a small peak for  $V^V$  but 97% of the spectral intensity is in the  $V^{IV}$  peak at 2500 ppm. Promotion with Cr leads to an increase in the fraction of  $V^V$ , which amounts to 12% of the signal intensity. Promotion with Fe produces a sample with essentially no  $V^V$  after activation. After use in methane oxidation, the unpromoted and Fe-promoted samples exhibit increased  $V^V$  signals, 6% for

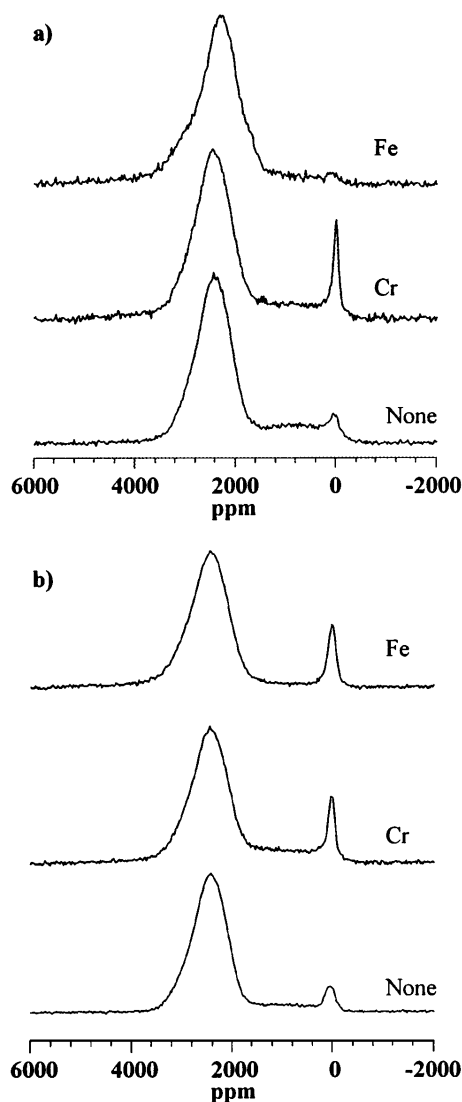


FIG. 2. Wideline  $^{31}P$  NMR spectra of promoted and unpromoted vanadyl pyrophosphate: (a) freshly activated in butane/air; (b) after 20 h use in methane oxidation.

unpromoted and 10% of signal intensity for Fe-promoted. The spectrum of the Cr-promoted sample is essentially unchanged at 12%  $V^V$ . Average vanadium oxidation state estimated by integration of the NMR peak intensities are reported in Table 2 for comparison with XPS values. The NMR (bulk) values are slightly lower than the XPS (surface) values determined using the deconvolution approach. However, the results are consistent with the XPS and XRD data, which indicate that promoters enhance the concentration of  $V^V$  or oxidized VPO phases, even under the highly reducing conditions employed for methane oxidation.

Diffuse reflectance infrared spectra were obtained for both promoted and unpromoted catalysts. Band positions in the 700 to 1700  $cm^{-1}$  range agreed closely with those

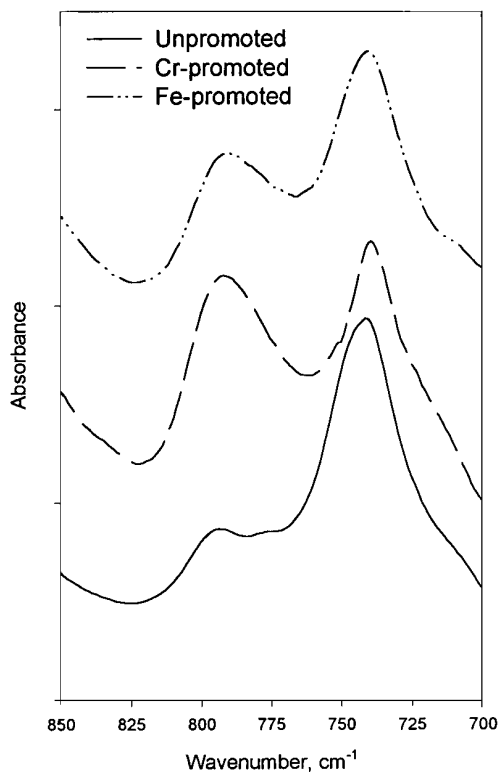


FIG. 3. Infrared spectra (diffuse reflectance) showing the P–O–P symmetric stretch at  $742\text{ cm}^{-1}$  and the V–(O=V) stretch at  $795\text{ cm}^{-1}$ .

reported by others for vanadyl pyrophosphate (9, 25) with an absorbance maximum at  $975\text{ cm}^{-1}$  assigned to V=O stretching. This intense band was broad and not well resolved in these samples. The only significant differences observed in the spectra are for vibrations of the linkages between the layers of the  $(\text{VO})_2\text{P}_2\text{O}_7$  structure and this region of the spectrum is shown in Fig. 3. For the Cr- and Fe-promoted catalysts the (V=O)–V band at  $795\text{ cm}^{-1}$  has a greater intensity relative to the P–O–P band at  $742\text{ cm}^{-1}$  than is observed in the unpromoted catalyst. Examination of the entire infrared spectrum suggests that the band at  $742\text{ cm}^{-1}$ , corresponding to the P–O–P stretch, has decreased in intensity. Thus the promoter atoms are somehow affecting the layer linkages, perhaps by becoming intercalated between the layers. This intercalation, if it occurs, does not appear to have produced disorder in the layer stacking as shown by XRD. Ordering and crystallinity may have actually increased for the Fe-promoted sample.

#### Catalyst Testing

Prior to any measurement, the contribution of gas phase reactions was evaluated by performing a series of experiments with the empty reactor packed with quartz beads. In the absence of a catalyst and at the temperatures and flow rates employed in the present work, conversions of methane, methanol, and formaldehyde were negligible as

reported elsewhere (32). Consequently, the observations in the presence of catalyst appear to be primarily the result of heterogeneous process with very little or no intrusion of purely gas phase reactions. A number of experiments and calculations were performed to ensure that the measured reaction rates were not confounded by mass transfer effects (33). Experiments varying catalyst particle size and varying gas velocity at constant space velocity indicate no internal or external limitations. Calculations indicate that at  $698\text{ K}$ , the highest temperature employed in this study, the isothermal effectiveness factor is greater than 0.95.

**Unpromoted VPO.** The principal products of methane oxidation over VPO were found to be carbon monoxide and carbon dioxide. Formaldehyde was found only in trace quantities. Figure 4 presents selectivities to these products as a function of conversion, varied by varying temperature and GHSV for two different methane to oxygen ratios. As shown, carbon monoxide is the primary product and CO selectivity decreases as the conversion increases. At zero conversion, CO selectivity approaches 100% suggesting that methane is oxidized directly to carbon monoxide and that any methoxy or formate surface intermediate is very rapidly converted under these conditions. Carbon dioxide was never a significant product at very low methane conversion levels, which is an indication of no direct oxidation route from methane to carbon dioxide. CO selectivity is higher at the higher methane to oxygen ratio, as expected because less oxygen is available.

To determine the reaction orders, methane partial pressure was changed from 21 to 65 kPa, keeping the oxygen partial pressure constant at 8 kPa. During these runs, gas hourly space velocity (GHSV) was also kept constant at  $2700\text{ h}^{-1}$ . In a similar set of experiments at the same GHSV

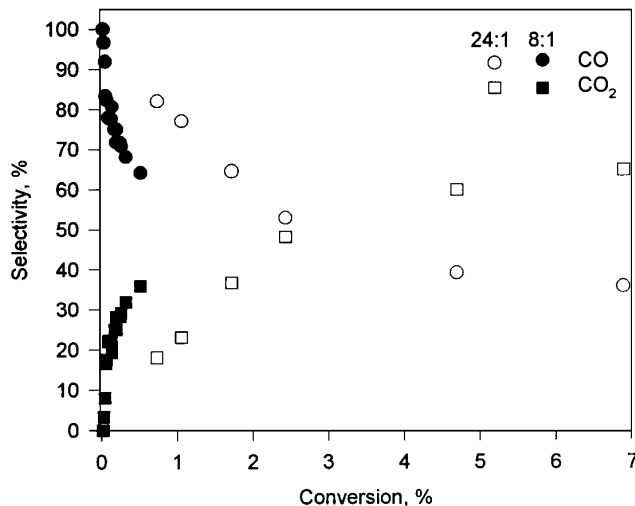


FIG. 4. Product selectivity (%) as a function of methane conversion (%) for unpromoted vanadyl pyrophosphate catalyst. GHSV =  $2700\text{--}13,500\text{ h}^{-1}$ ,  $P_{\text{CH}_4} = 43\text{ kPa}$ ,  $P_{\text{O}_2} = 5\text{ kPa}$ ,  $T = 573\text{--}698\text{ K}$ .

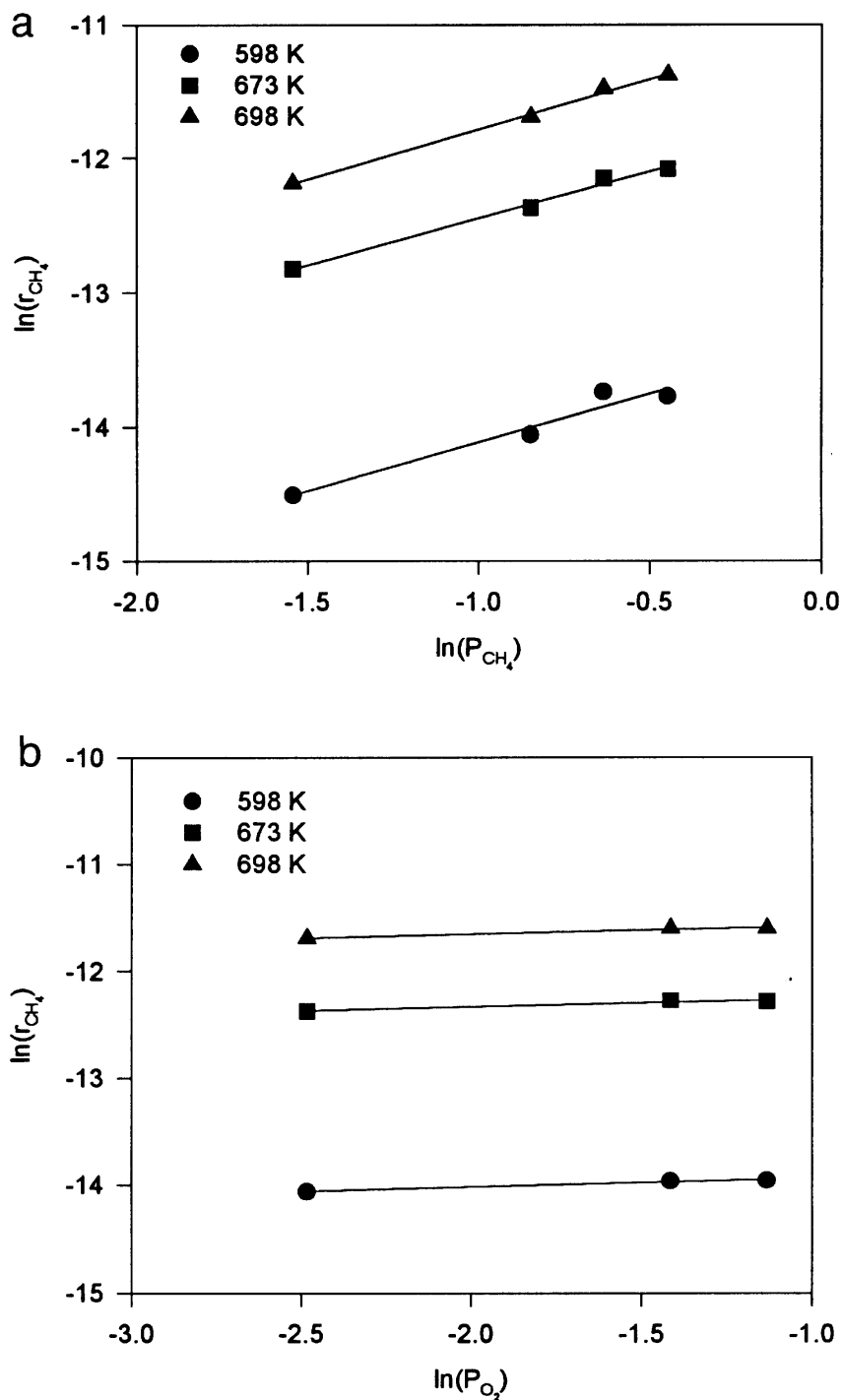


FIG. 5. Effect of (a) methane partial pressure and (b) oxygen partial pressure on methane oxidation rate over unpromoted VPO.

oxygen partial pressure was changed from 8 to 32 kPa, keeping methane pressure constant at 42 kPa. The effect of reactant partial pressures on the observed rate is shown in Fig. 5. The data indicate that the reaction order for methane was  $0.73 \pm 0.07$  (indicated confidence intervals are standard error). The rate of reaction of methane showed a very small

positive order in oxygen of about  $0.08 \pm 0.02$ , provided that oxygen conversion was kept below 100%. Both reaction orders were not affected by temperature over the range studied.

Temperature dependence of the rate was determined by varying the temperature between 583 and 713 K. An

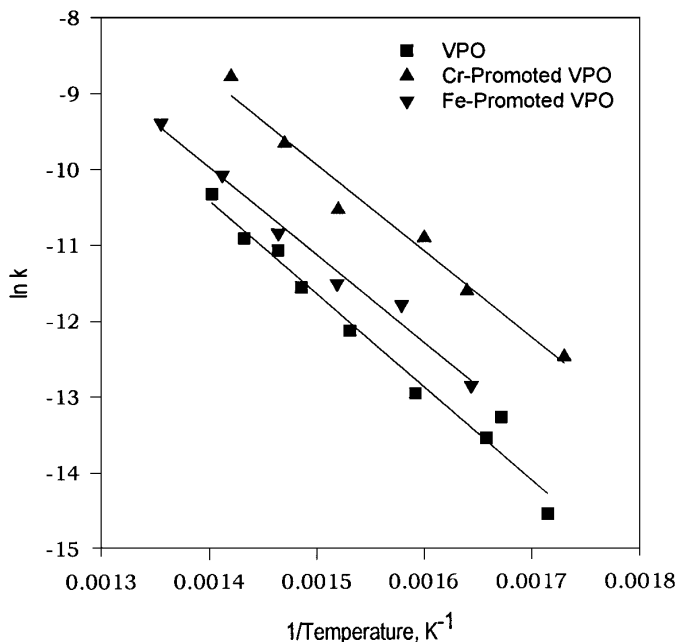


FIG. 6. Arrhenius plot for methane oxidation reaction over promoted and unpromoted vanadyl pyrophosphate.

Arrhenius plot is shown in Fig. 6. The linear nature of this plot, even at the highest conversions (in all cases well below 10%) and temperatures confirms the absence of significant mass transfer limitations in this system. An activation energy of  $102 \pm 6$  kJ/mole is calculated for methane conversion. Arrhenius parameters are summarized in Table 3.

*Transition metal-promoted catalysts.* Methane oxidation over the Cr- and Fe-promoted VPO catalysts was carried out at a fixed GHSV of  $9300 \text{ h}^{-1}$  and at a methane-to-oxygen ratio of 8.3. Selectivity as a function of methane conversion for these catalysts is shown in Fig. 7. Formaldehyde was observed as a significant product in the reactor effluent for both Fe- and Cr-promoted VPO catalysts. Admittedly, conversions are very low in these experiments and not significant in an applied sense. However, the point to be made is that in repeated experiments, no formaldehyde was observed over the unpromoted catalysts under nearly identical reaction conditions (lowest conversions in Fig. 4), but formaldehyde was observed over the promoted samples.

TABLE 3

Arrhenius Parameters for Methane Oxidation over Promoted and Unpromoted VPO Catalysts

Catalyst	Activation energy, kJ/mole	Preexponential factor, mole/g-min-atm <sup>0.81</sup>
VPO	$102 \pm 6$	860
Cr-VPO	$95 \pm 8$	1273
Fe-VPO	$96 \pm 6$	505

Large (up to  $5 \text{ cm}^3$ ) GC sample loops were employed to amplify the formaldehyde signal in these runs. Formaldehyde peaks were five to six times greater than the noise level. Individual analyses as well as entire experiments were repeated with essentially the same results to within 10%.

In both promoted catalysts, at zero conversion formaldehyde selectivity approaches 100%, suggesting that it is the primary reaction product. Formaldehyde selectivity decreases rapidly as the extent of reaction increases. The increase in selectivity to carbon monoxide indicates that this compound is produced upon further oxidation of formaldehyde. Carbon dioxide became the principal product at higher conversions. No  $\text{CO}_2$  formation at low conversions indicates no direct oxidation route from methane to carbon dioxide. Assuming that the rate of methane oxidation has

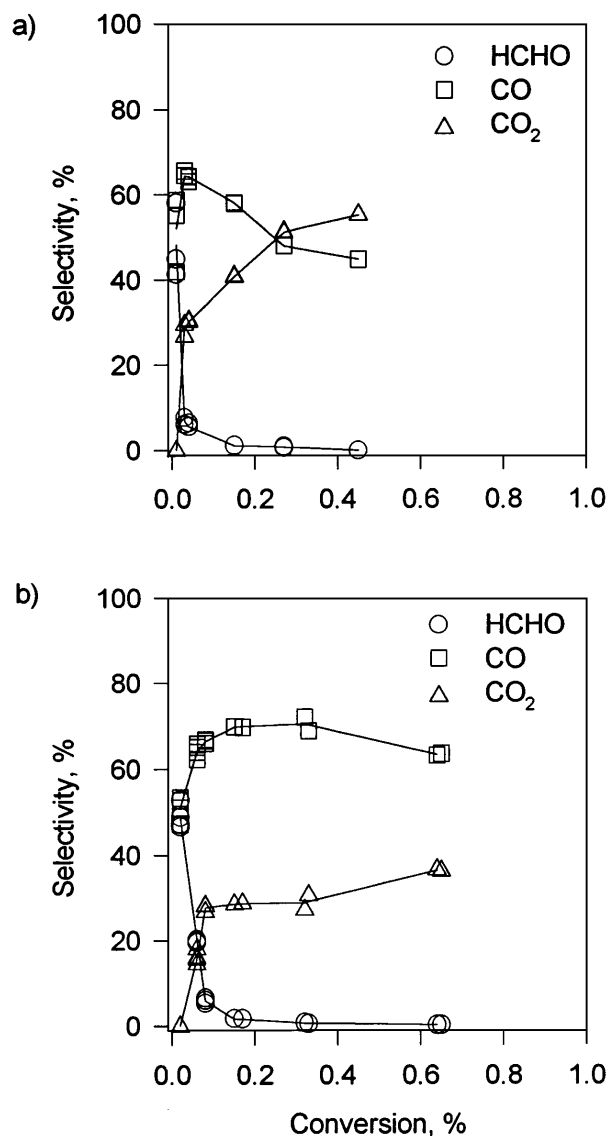
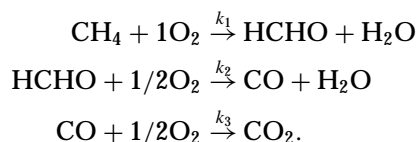


FIG. 7. Product selectivity (%) as a function of methane conversion (%) for promoted vanadyl pyrophosphate catalysts: (a) Cr; (b) Fe.

the same dependency on methane and oxygen partial pressures as the unpromoted catalyst, the Arrhenius relationships in Fig. 6 were drawn and the Arrhenius parameters are listed in Table 3. Activation energies are essentially the same for the unpromoted, Fe- and Cr-promoted catalysts.

### DISCUSSION

The catalyst testing data indicate a sequential reaction path for methane oxidation over VPO and the promoted catalysts, as has also been reported for methane oxidation over  $V_2O_5/SiO_2$  (34) and other catalysts:



Unpromoted vanadyl pyrophosphate is a poorly selective partial oxidation catalyst for the methane oxidation reaction. Carbon oxides and water are the principal products, indicating that the ratio  $k_2/k_1$  is large. A fractional order of 0.73 in methane partial pressure was observed. In the literature, with few exceptions, methane partial oxidation is assumed to be first order in methane and zero order in oxygen. Notably, Wang and Otsuka (30) recently reported data that we have analyzed to yield a 0.68 order for methane oxidation over  $FePO_4$  in the presence of hydrogen. A reaction order below unity indicates the existence of an inhibition (adsorption) term in a Langmuir-Hinshelwood-type rate model. We interpret this to mean that as  $P_{CH_4}$  increases, the surface becomes more reduced and sites capable of catalyzing oxidation become fewer. The reaction order for oxygen was found to be 0.08, very close to zero, as expected for a redox or Mars and van Krevelen process with fast catalyst reoxidation. Promotion of VPO with Fe or Cr leads to the formation of measurable quantities of formaldehyde, although space-time yields are low, typically between 0.5 and 2 g/kg-h. Low reaction temperatures and operation at very low methane conversion are required for formation of HCHO.

Activation energy values for methane oxidation over several different oxide catalysts have been listed in Table 4. Typical oxide catalysts exhibit activation energies for methane oxidation that are 1.5 to 2 times higher than observed for VPO, although much of this data is based on  $N_2O$  as the oxidant. An exception is 12-molybdophosphoric acid studied by Ahmed and Moffat (35) which exhibits an activation energy similar to that reported here. Busca and co-workers (17) have proposed that strong surface acid sites are involved in the initial alkane activation step. We speculate that a surface acid site is involved in methane activation, and because of the strongly acidic nature of vanadyl pyrophosphate and 12-molybdophosphoric acid, the activation energy for methane oxidation has a lower value.

**TABLE 4**  
Comparison of Methane Oxidation Activation Energies Reported for Various Catalysts

Reference	Catalyst	Activation energy, kJ/mole
30	$FePO_4$	205
34	$V_2O_5-SiO_2$	226
35	$H_3PMo_{12}O_{40-x}H_2O$	113 <sup>a</sup>
36	$MoO_3-SiO_2$	188
37	$MoO_3$	167 <sup>a</sup>
38	$(MoO_3)_3-Fe_2O_3$	176
39	$V_2O_5-SiO_2$	251
40	$V_2O_5-Al_2O_3$	188
40	$MoO_3-SiO_2$	176 <sup>a</sup>
41	$V_2O_5-SiO_2$	167 <sup>a</sup>
42	Silica	154
42	Vycor	217

<sup>a</sup> Nitrous oxide as the oxidizing agent.

Characterization of promoted catalysts indicates that promoter elements are present on the surface and in the bulk at roughly 10:1 vanadium to promoter ratio. XRD indicates that vanadyl pyrophosphate is the main phase present, but promotion has resulted in several new peaks in the powder pattern, several of which can be assigned to  $\alpha_{II}-VOPO_4$ . Examination of the (200) reflection at about  $22.8^\circ$  2-theta suggests that promotion has not generated additional disorder (additional peak broadening) in the layer stacking and may have actually enhanced crystallinity in the Fe-promoted sample. Promotion appears to increase the average oxidation state (surface and bulk) of vanadium and, based on the IR spectral data, disrupts linkages between the layers of the structure.

We hypothesize that promoter atoms are incorporated between the layers and at the edges of the layers of these crystals rather than substituting for vanadium in the phosphate lattice. This is consistent with the method of promoter addition where promoters were added to the fully formed precursor. Perhaps the presence of these cations increases the degree of coordinative unsaturation of the surface vanadium centers favoring formation of oxidized vanadium as isolated  $V^V$ , or as  $V^V$  containing phase domains. Alternatively, promoters might activate oxygen more readily than VPO and catalyze oxidation of  $V^{IV}$  to form  $V^V$ . If promoter atoms are indeed at the edges of, or in between, the vanadyl pyrophosphate layers the promoter may enhance the ability of the structure to incorporate additional oxygen between the layers resulting in formation of  $V^V$ . A model where excess oxygen is incorporated between the layers has been discussed by Lopez Granados and co-workers (9).

The presence of  $V^V$  is, of course, necessary for operation of a  $V^{IV}/V^V$  redox couple. Under butane oxidation conditions (1.5% butane in air) excess oxygen is present and the formation of  $V^V$  sites or phase domains is facile (11, 12).

Furthermore, using *in situ* Raman studies of VPO activation in butane/air, Hutchings and co-workers (43) observed the formation of  $V^V$  phases simultaneously with the start of maleic anhydride formation. Over the course of 20 h the concentration of these phases increased, as did the selectivity to maleic anhydride. In a more recent *in situ* X-ray absorption spectroscopy study, Coulston and co-workers (6) concluded that  $V^V$  was involved in the reaction to form maleic anhydride and that  $V^{IV}$  was involved in reactions to form by-products. Production of maleic anhydride ended with removal of  $V^V$  from the catalyst by reduction and reaction of  $V^{IV}$  produced only carbon oxides. Thus there is considerable evidence that  $V^V$  species are necessary to form selective products under butane oxidation conditions.

Under methane oxidation conditions (in the range of 90% methane and 10% oxygen) there is no excess oxygen and formation of  $V^V$  may be unfavorable in unpromoted catalysts. The observation that the reaction order with respect to methane is less than unity may imply a loss of  $V^V$  sites capable of catalyzing oxidation as methane partial pressure is increased. Unfortunately, reaction order with respect to methane was not measured for the promoted catalysts. Promotion with Fe or Cr appears to stabilize or enhance the formation of  $V^V$ , as isolated sites or oxidized phase domains, and this may be responsible for the improved selectivity to partial oxidation products. Ben Abdelouahab and co-workers (44) have reported a similar effect in butane oxidation for promotion by Fe and Co which were added as acetylacetonate salts during precursor preparation. Promotion enhanced the formation of a  $VOPO_4$  structure at lower temperatures and resulted in improved selectivity to maleic anhydride. While yields of selective oxidation products are quite low in the present study, the selectivity and characterization results support the notion that  $V^V$  is a necessary component of VPO surface sites capable of selectively oxidizing alkanes.

## ACKNOWLEDGMENTS

This work was sponsored by the U.S. Department of Energy, Fossil Energy Branch, under Contract DE-AC22-96PC92110. Acquisition of the solid state NMR instrument was sponsored by the National Science Foundation under Award CTS-9512228.

## REFERENCES

- Poirer, M. G., Sanger, A. R., and Smith, K. J., *Canad. J. Chem. Eng.* **69**, 1027 (1991).
- Hall, T. J., Hargreaves, J. S. J., Hutchings, G. J., Joyner, R. W., and Taylor, S. H., *Fuel Proc. Technol.* **42**, 151 (1995).
- Parkyn, N. D., Warburton, C. I., and Wilson, J. D., *Catal. Today* **18**, 385 (1993).
- Brown, M. J., and Parkyn, N. D., *Catal. Today* **8**, 305 (1991).
- Centi, G., Trifiro, F., Ebner, J. R., and Franchetti, V. M., *Chem. Rev.* **88**, 55 (1988).
- Coulston, G. W., Bare, S. R., Kung, H., Birkeland, K., Bethke, G. K., Harlow, R., Herron, N., and Lee, P. L., *Science* **275**, 191 (1997).
- Li, J., Lashier, M. E., Schrader, G. L., and Gerstein, B. C., *Appl. Catal.* **73**, 83 (1991).
- Ben Abdelouahab, F., Olier, R., Guilhaume, N., Lefebvre, F., and Volta, J. C., *J. Catal.* **134**, 151 (1992).
- Lopez Granados, M., Conesa, J. C., and Fernandez-Garcia, M., *J. Catal.* **141**, 671 (1993).
- Sananes, M. T., Tuel, A., Hutchings, G. J., and Volta, J. C., *J. Catal.* **148**, 395 (1994).
- Zhang-Lin, Y., Forissier, M., Vedrine, J. C., and Volta, J. C., *J. Catal.* **145**, 267 (1994).
- Kiely, C. J., Burrows, A., Sajip, S., Hutchings, G. J., Sananes, M. T., Tuel, A., and Volta, J. C., *J. Catal.* **162**, 31 (1996).
- Michalakos, P. M., Kung, M. C., Jahan, I., and Kung, H. H., *J. Catal.* **140**, 226 (1993).
- Ai, M., *J. Catal.* **101**, 389 (1986).
- Busca, G., and Centi, G., *J. Am. Chem. Soc.* **111**, 46 (1989).
- Kung, H. H., *Indus. Eng. Chem. Prod. Res. Dev.* **25**, 171 (1986).
- Busca, G., Centi, G., Trifiro, F., and Lorenzelli, V., *J. Phys. Chem.* **90**, 1337 (1986).
- Hodnett, B. K., *Catal. Rev.-Sci. Eng.* **27**, 373 (1985).
- Lopez Granados, M., and Wolf, E. E., *Appl. Catal. A: General* **131**, 263 (1995).
- Hutchings, G. J., *Appl. Catal.* **72**, 1 (1991).
- Otake, M., U.S. Patent 4,337,173 (January 29, 1982).
- Takita, Y., Tanaka, K., Ichimaru, S., Mizihara, Y., Abe, Y., and Ishihara, T., *Appl. Catal. A: General* **103**, 281 (1993).
- Hutchings, G. J., and Higgins, R., *J. Catal.* **162**, 153 (1996).
- Sananes-Schulz, M. T., Ben Abdelouahab, F., Hutchings, G. J., and Volta, J. C., *J. Catal.* **163**, 346 (1996).
- Busca, G., Cavani, F., Centi, G., and Trifiro, F., *J. Catal.* **99**, 400 (1986).
- Cornaglia, L. M., and Lombardo, E. A., *Appl. Catal. A: General* **127**, 125 (1995).
- Moser, T. P., and Schrader, G. L., *J. Catal.* **104**, 99 (1987).
- Garbassi, F., Bart, J., Tassinari, R., Vlaic, G., and Laborde, P., *J. Catal.* **98**, 317 (1986).
- Coulston, G. W., Thompson, E. A., and Herron, N., *J. Catal.* **163**, 122 (1996).
- Wang, Y., and Otsuka, K., *J. Catal.* **15**, 256 (1995).
- Watson, I. M., Connor, J. A., and Whyman, R., *Thin Solid Films* **201**, 337 (1991).
- McCormick, R. L., in "Proceedings: Coal Liquefaction and Gas Conversion Contractors Review Conference, August 29-31, 1995, Pittsburgh, PA," p. 591.
- Alptekin, G. O., Ph.D. thesis, Department of Chemical Engineering and Petroleum Refining, Colorado School of Mines, Golden, CO, in preparation.
- Spencer, N. D., and Pereira, C. J., *J. Catal.* **116**, 399 (1989).
- Ahmed, S., and Moffat, J. B., *Appl. Catal. A: General* **40**, 101 (1988).
- Spencer, N., *J. Catal.* **109**, 187 (1988).
- Khan, M. M., and Somorjai, G. A., *J. Catal.* **91**, 263 (1985).
- Chellappa, A. S., and Viswanath, D. S., *Indus. Eng. Chem. Res.* **34**, 1933 (1995).
- Koranne, M. M., Goodwin, J. G., and Marcelin, G., *ACS Div. Petr. Chem. Prepr.* **37**(1), 41 (1992).
- Liu, H.-F., Liu, R.-S., Liew, K. Y., Johnson, R. E., and Lunsford, J. H., *J. Am. Chem. Soc.* **106**, 4117 (1984).
- Zhen, K. J., Khan, M. M., Mak, C. H., Lewis, K. B., and Somorjai, G. A., *J. Catal.* **94**, 501 (1985).
- Kastanas, G. N., Tsigdinos, G. A., and Schwank, J., *ACS Div. Petr. Chem. Prepr.* **33**(3), 393 (1988).
- Hutchings, G. J., Desmartin-Chomel, A., Olier, R., and Volta, J.-C., *Nature* **368**, 41 (1994).
- Ben Abdelouahab, F., Olier, R., Ziyad, M., and Volta, J. C., *J. Catal.* **157**, 687 (1995).